Computational study of contact patterns in the ankle joint after ligamentous injury

Gonçalo Ribeiro Lopes Rodrigues Marta
goncalo.marta@tecnico.ulisboa.pt

Instituto Superior Técnico, Lisboa, Portugal

October 2018

Abstract

The ankle is a complex joint, with the ligaments as its main stabilizer, which when injured, induce instability and a change in the cartilaginous contact pressures. The main goal of this work is to study the changes in those contact pressures as well as the changes in the ligamentous strain and in the ankle reaction moments, using the finite element method (FEM).

This work involved the creation of the (FEM) of the ankle joint (AJ), namely of its mechanical properties and boundary conditions. Three internal rotation (IR) levels, experimentally measured, were applied in the ankle for three different ligamentous configurations.

The results show a high strain rate at the anterior talofibular ligament (ATFL) and at the posterior tibiotalar ligament (PTTL), denoting their importance in the ankle's (IR). There is also not only an increase of the maximum pressure in the ankle cartilage but also the occurrence of pressure spots at the anteromedial and posterolateral areas of the talar cartilage, possible precursors of cartilaginous injuries with degenerative implications.

Keywords: Ankle joint; Contact pressures; Ligaments; Finite Element Method.

1. Introduction

The AJ is a very complex system composed of three individual joints: the tibiotalar (TT), the talofibular (TaFi) and the tibiofibular (TiFi), acting as a link between the leg and the foot. Both the anatomical and biomechanical characteristics of the ankle joint allow it to be a major weight-bearer in all of the daily activities, transferring the loads between the leg and the foot. This characteristic is highly important since the foot is the basis used by the body to stand, walk and run and the loads generated in these activities are all partially supported by the AJ [1].

The complexity of the AJ and the large forces applied in the legs and feet lead to a high incidence of injuries, with ankle sprains (AS) and arthritis being the ones with the higher occurrence rate. In fact in a study made by Yung et al. [2], ankle injuries are ranked the most popular injured body site with 34.3% of all injuries, followed by knee injuries. Among ankle injuries, ankle sprains are the most common.

An AS happens when ligaments supporting the ankle stretch beyond their limits and tear with 3 possible severity degrees [3]. The diagnosis and injury quantification for AS, however, depend highly on the mobilization made by the orthopedist, which is very subjective [4].

Arthritis is a pathology that disrupts the normal function of joints by destroying their articular surface. The two forms of arthritis that are most common are osteoarthritis (OA) and rheumathoid arthritis [5]. OA develops in joints that are injured or that are repeatedly overused, wearing the cartilage at the end of the bones. If the cartilage damage occurs after trauma it is called secondary OA [5]. On the other side, rheumathoid arthritis is an autoimmune inflammatory disease, in which the body releases a group of enzymes that destroy the cartilage of joints [6]. Many authors establish a correlation between ligamentous injuries and a progressive degenerative arthritis of the ankle joint [7, 8]. Taga et al.[9] examined arthroscopically both stable and unstable ankles, and observed that for stable ankles - or ankles that underwent any kind of ligamentous reconstruction after lateral collateral ligament (LCL) injury - the cartilage damage was not as proeminent as the damage observed in unstable ankles, which had high wear rates especially in the medial side of the tibial and talar cartilage. An association between (LCL) injury and cartilage lesion was then established.

The main goal of this work is to simulate 3 angles of internal rotation (IR) of the ankle for 3 differ-

ent ligamentous configurations - based on the work done by Guerra-Pinto et al. [4], in which the ankle rotational instability is tested after the cut of successive (LCL) - and extract not only the strain felt by each ligament during the rotation but also the cartilage pressure in the ankle cartilages and the reaction moments applied on the model. For this purpose, a finite element (FE) model of the AJ, with appropriate mechanical properties and boundary conditions is developed.

2. Background

An AS happens when there is a forced movement in the ankle, causing injury to the ligaments. There are some predisposing factors to this type of injury, such as muscular exhaustion, ligamentous laxity and neurological changes including proprioceptive deficit caused by previous trauma. One of the main problems that can arise from successive AS is chronical instability. The treatment for AS includes surgery for ligament repair, balance training to help stabilize the joint and functional treatment using bandages or tape [10]. Zwipp et al. [11], in 1985-1986 tried to determine the best treatment for ruptured ankle ligaments, comparing surgery combined with immobilization or functional treatment and a conservative approach (without surgery), but the study was inconclusive since all the approaches were equally effective.

Hence there seems to be a *status quo* in terms of treatment for ligament rupture. However, the diagnostic is still quite subjective and there are no standardized examination procedures or evidence-based treatments. Moreover, imagiology processes can help on the diagnosis but they represent extra costs [12]. Regarding the tests to evaluate ankle injuries, the anterior drawer test consists in, pressing the heel forward, with the knee joint flexed, while holding the tibia back. This test is used to evaluate the extension of the injury on the ATFL. On the other hand, the talar tilt is used to assess the injury extension on the calcaneofibular ligament (CFL) and on the ATFL. The test consists on inverting the talus and the calcaneus on the tibia.

These maneuvers are, nevertheless, associated with a high variability in its sensitivity [4], being the reason why a new approach to the clinical diagnosis needs to be developed. The work from Guerra-Pinto et al. [4], which comes to alter the paradigm for the diagnosis of ligament injury - and is the starting point for this thesis -, is based on the hypothesis that a sequential sectioning of the lateral ligaments of the ankle results in a progressive angular ankle laxity when an internal rotation is applied, resulting in a completely different approach to the diagnosis phase. Guerra et al. found that the ankle would increase almost threefold the IR after single ATFL cut and almost fourfold after ATFL and CFL cut. With these findings, they were able to conclude that this evidence of rotational laxity was a major step to define a new diagnostic method for LCL injury, avoiding further inconsistencies and variability in its diagnosis.

Until now, the FE models existent were used to model the ankle in physiological conditions, or with small changes to that condition, simulating only particular injuries. Moreover, studies regarding ankle instability were not found in the literature, with this work being very important to clarify the implications of ligamentar injury on the ankle cartilaginous pressure patterns, particularly of the rotational instability caused by the LCL injury. This ankle instability due to ligamentar injury, has proven to be a precursor of cartilaginous alterations, which can lead to OA over time [13].

3. Methods

The 3D modelling of the bones starts with a acquisition of a CT scan from the region of interest. Segmentation of the bones was performed in ITK-SNAP® (version 3.6.0, 2017) software. After the segmentation process, a surface model of the tibia, fibula, talus, calcaneus, navicular and cuboid was created and imported into MeshLab [14] for data filtering using a Laplacian smoothening filter. The solid model was created in SolidWorks® (Student Edition, Academic Year 2016-2017), where the the proximal ends of both the tibia and fibula were cut using the same plane, not being taken into account for the subsequent simulations. The fibular and tibial cartilages were generated by extruding their surface mesh by 0.7 mm and 1 mm respectively. The talar cartilage was created by scaling up the talus 1.2 times its original size and then subtract the normal-sized bone, creating a shell with the desired thickness - 1.5 mm. The choice of the nine ligaments used came from the study of Rasmussen et al. [15] about the stability of the ankle joint, the study from Corazza et al. [16] and the work from Guerra Pinto [4]. Three medial collateral ligaments - PTTL, anterior tibiotalar ligament (ATTL) and tibionavicular ligament (TiNL) -, three LCL - posterior talofibular ligament (PTFL), ATFL and CFL - and three other ligaments - calcaneonavicular ligament (CNL), cuboideonavicular ligament (CuNL) and the calcaneocuboid ligament (CaCL) - were modelled using tension only truss elements. Their insertion areas were created based on anatomical descriptions and medical images [17], and their endings were coupled to the attachment surfaces, uniformly distributing the forces applied in those surfaces.

Table 1: Mechanical properties for all the ligaments considered in this work, as well as the cross-sectional area for each ligament. The material properties were taken from Corazza et al., Liacouras et al., Siegler et al. and Cheung et al. [16, 18, 21, 22].

Ligament	Young's Modulus, E (MPa)	Poisson's Ratio, ν	Cross-sectional area (mm^2)
ATFL	225.5	0.46	12.9
PTFL	216.5	0.46	21.9
CFL	512	0.46	9.7
TiNL	320.7	0.46	7.1
ATTL	184.5	0.46	13.5
PTTL	99.54	0.46	45.2
CNL	260	0.46	0.7
CuNL	260	0.46	105
CaCL	260	0.46	98.67

3.1. Material Properties

In this work, bone was assigned an Young's modulus of 7.3 GPa and a Poisson's ratio of 0.3 according to Cheung et al. and Gefen et al. [18, 19]. Cartilage has a viscoelastic behaviour [20], but was modelled here using a linear elastic and isotropic law with a Young's modulus and Poisson's ratio of 10 MPa and 0.4 [19] - due to its almost incompressible nature. The ligaments were considered to have different Young's moduli and cross sectional areas, but the same Poisson's ratio. The values considered were taken from the works of Corazza et al., Liacouras et al., Siegler et al. and Cheung et al. [16, 18, 21, 22]. No data were found for the CNL, the CuNL and the CaCL. However, the value of 260 MPa was used accordingly to the work done by Ozen et al.[23], and the cross-sectional area was calculated using the relationship between a spring's constant of a rod and the Young's modulus of that same rod:

$$k = Y\frac{A}{L} \tag{1}$$

where k is the spring's constant - assumed to be 70 N/mm according to the work of Liacouras et al. [21] -, Y is the Young's modulus, A is the cross-sectional area and L is the length of the ligament. In terms of Poisson's ratio, all ligaments were assumed to be incompressible, assuming ν =0.46. The mechanical properties for all ligaments are presented in Table 1.

To the ligaments modelled, a 2% prestrech was applied to represent in situ levels [21].

3.2. Model Definition

The interactions between bone and cartilage were considered rigidely bonded using a tie constraint. Cartilage on cartilage interactions were simulated using a surface-to-surface contact formulation. Because the interaction between articular surfaces can be considered almost frictionless [23], a coefficient of friction of 0.01 was considered [24].

The main focus of this work is the IR of the AJ joint. Nevertheless, the presence of a compressive force to induce the contact of the cartilages is required. Therefore, a compressive force of 10 N was applied.

Before assigning all the boundary conditions, the axis about which the rotation will be performed, must be defined. This was attained by creating a main axis (MA) that resembled the longitudinal rod which served as pivot in the work of Guerra-Pinto et al.[4]. This MA went through the plantar area of the foot, 0.5cm away from the medial shoulder of the talus and through the distal aspect of the tibia, in line with its sagittal and coronal axis.

The tibia and fibula were fixed in their proximal surface and the tarsal bones - talus, calcaneus, navicular and cuboid - were defined as rigid bodies using a rigid body constraint. To constraint the movement of the rigid bodies, the reference point controlling the rigid bodies was constrained to allow only their translation along the MA direction and their rotation about the same axis.

As described earlier, there are 3 cases of rotation for 3 different ligamentous configurations. The loading conditions were applied in two steps. In the first step, only the compressive load of 10 N was considered, and the rigid body reference point could only move in the direction of the MA. The second step included also the compressive force of 10 N, but an IR around the MA was applied, depending on the ligamentous configuration - 3.67°for the intact ankle, 9.6°after ATFL section and 13.43°after ATFL and CFL section.

Bone was meshed using tetrahedral elements (C3D4) with 1.0 mm size [25] whereas cartilage, and to enhance results accuracy, was meshed using hexahedral elements (C3D8) with 0.5 mm size. Ligaments were meshed using a linear truss mesh with the size equal to the size of the ligament.

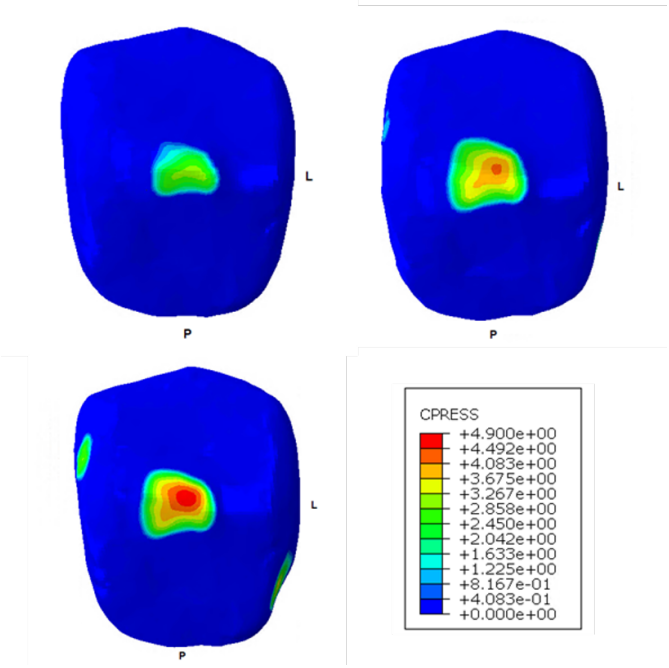

Figure 1: Contact pressures (MPa) in the talar cartilage for IR of 3.67°in the top left, for an IR of 9.6°in the top right and for an IR of 13.43°in the down left. P and L stand for posterior and lateral respectively

3.3. Results Presentation

In this work, the contact pressure, the ligamentous strains and the reaction moments were calculated and analyzed.

Contact pressure was extracted for each cartilage - talar, tibial and fibular - and only the maximum pressures are highlighted.

Ligamentous strains were calculated by evaluating the initial size of the ligaments before and after rotation and computing the Cauchy strain formula:

$$\varepsilon = \frac{\Delta L}{L} = \frac{l - L}{L}, \tag{2}$$

where ε represents the strain of the ligament, L is the initial size of the ligament and l is the final size of the ligament.

Reaction moments, which are the reactions induced by the ligaments and the cartilaginous contact after the ankle rotation, were extracted for the entire model and only the reaction moment around the MA was considered.

4. Results and Discussion

4.1. Cartilage Pressure

The computed contact pressures for the talar cartilages are displayed in Figure 3. Three rotational conditions are considered in this analysis. The results show not only a change on the contact pressure patterns with the different angles of IR, but also a growth of the maximum pressure felt in every cartilage.

Comparing qualitatively the contact areas on the talar cartilage, a continuous increase is observed from 3.67°to 13.43°of IR.

Table 2: Values for the maximum pressure (MPA) on the fibular, tibial and talar cartilages for IRs of 3.67°, 9.6°and 13.43°.

	3.67°	**9.6°**	**13.43°**
Fibular cartilage	-	2.23	3.63
Tibial cartilage	3.09	4.15	4.75
Talar cartilage	3.11	4.15	4.77

There is also an occurrence of pressure "hot spots" in the anteromedial and posterolateral areas of the talar cartilage, coincident with pressure spots on the medial side of the tibial cartilage and on the fibular cartilage respectively.

The maximum pressures are in the range of 2.23-4.77 MPa, with the fibular cartilage having no pressure for an IR of 3.67°.

Regarding the contact pressures, a quantitative analysis was done by evaluating the maximum pressures for the three cases of rotation, which are presented in Table 2. The maximum pressures are in the range of 2.23-4.77 MPa, with the fibular cartilage having no pressure for an IR of 3.67°. By increasing the angle of IR, the maximum pressure also increases.

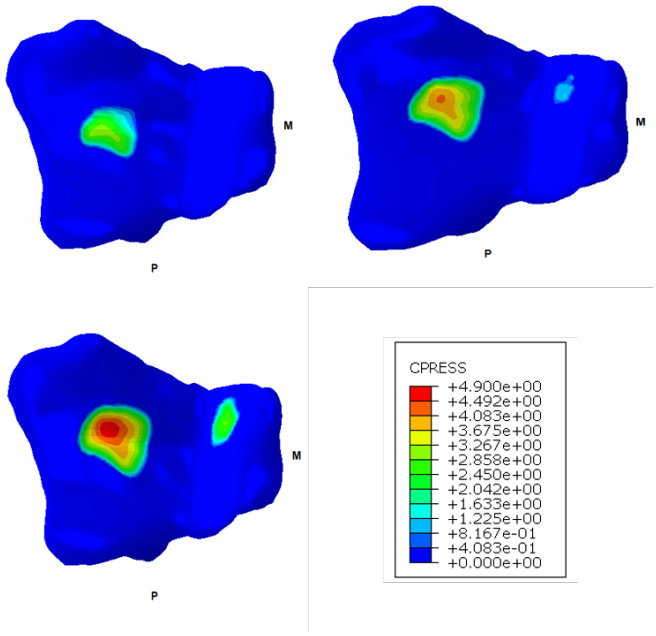

Figure 2: Contact pressures (MPa) in the tibial cartilage for IR of 3.67°in the top left, for an IR of 9.6°in the top right and for an IR of 13.43°in the down left. P and L stand for posterior and lateral respectively

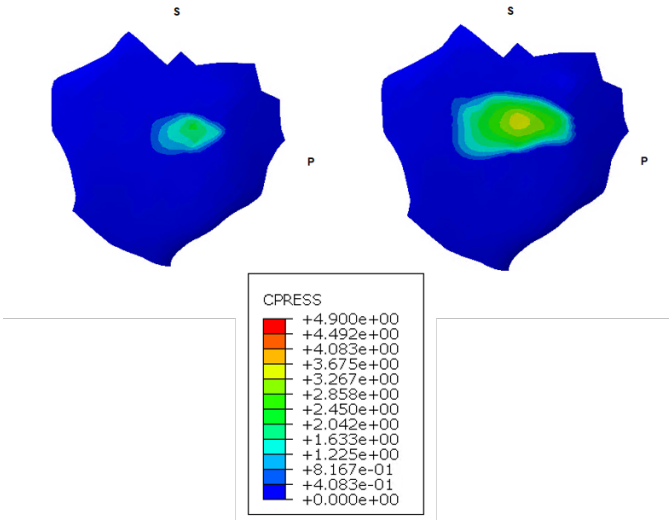

Figure 3: Contact pressures (MPa) in the fibular cartilage for IR of 9.6°in the top left and for an IR of 13.43°. P and L stand for posterior and lateral respectively

Table 3: Strains calculated for 5 ligaments - ATTL, PTTL, PTFL, CFL and ATFL - for the 3 degrees of rotation used in this work. Negative strains represent a shortening of the ligament whereas positive ones represent a stretching. The ATFL has been excluded from the 9.6% and 13.43% rotations and the CFL from the 13.43%, having no strains for that reason.

		Degrees of rotation		
		3.67°	**9.6°**	**13.43°**
Ligaments	**ATTL**	-3%	-7.2%	-9.2%
	PTTL	3.10%	8.7%	12.9%
	PTFL	-8.15%	-21.6%	-29.7%
	CFL	-2.8%	-4.5%	-
	ATFL	4.7%	-	-

4.2. Ligamentous Strains

To understand the ligamentar strain and consequent importance in the control of the IR, the strains of the ligaments present in this model were evaluated and compared with strains reported in the literature.

Table 3 contains the relevant strains retrieved from the FE model depending on the degree of IR.

According to Table 3, only the PTTL and the ATFL were stretched in the IR while all the other ligaments were shortened. In fact, the PTFL shortened 29.7%, being the ligament with the highest shortening, while the PTTL was the one with the highest stretching, with almost 13%, quadrupling the initial stretching value for 3.10%. The data for the ligaments not included in Table 4.2 are not presented because their strains were low.

4.3. Reaction Moments

The values for the reaction moments on the model can be seen in table 4. For this moments, IRs of 3.64°, 9.6°and 13.43°were applied for the models with intact ligaments, with ATFL cut and ATFL and CFL cut. The values presented were normalized by the reaction moment of the foot with intact ligaments and an IR of 3.64°.

The reaction moment increases with the rotation angle for the same ligamentous configuration and decreases with the cut of the ATFL for the same rotation angle. In fact, the value for the reaction moment for the model with intact ligaments increases almost 3.5 times from 3.67°to 9.6°and 1.8 times from 9.6°to 13.43°. The values for both the ATFL cut and a combination of ATFL and CFL cut are equal. For the same 3.67°of IR, both the models with the ATFL cut and ATFL and CFL cut produce a smaller reaction moment than the model with the intact ligaments. For both of these models, the reaction moments for 9.6°and 13.43°are 2.58 and 4.32 times higher than the reaction moment for the intact ligaments and 3.67°of IR. To summarize, using the same rotation angle, the reaction moment decreases with the cut of the ATFL, staying the same with the cut of the CFL. Additionally, considering the same ligamentous configuration, the reaction moment raises with the increasing of the IR angle.

4.4. Discussion

By observing both the tibial and talar pressure patterns in Figure 3, it is clear that for an healthy ankle, there are no pressure points in the medial facet of the tibial cartilage, as opposed to the pathological ankles. Clinical studies have shown that normal physiological loading does not harm the cartilage, since it responds in a very site-specific way to loads [26]. This can be explained due to a variation of the tensile modulus of an healthy human cartilage, depending on the location over the joint surface, meaning that high weight bearing regions have a higher tensile modulus and vice-versa [27]. Hence, cartilaginous areas that are not usually solicited by loads, will suffer lesions when abrupt, non-biological stresses are applied, such as the ones seen in the FE

Table 4: Values for the reaction moments (N m) taken from the FE model for the 3 rotation angles and for 3 different ligamentous configurations. Inside brackets are the normalized values by the reaction moment of the foot with intact ligaments and IR angle of 3.64°

Rotation Angle (°)	Intact ligaments	ATFL cut	ATFL and CFL cut
3.67	1.37(1)	1.27(0.93)	1.27(0.93)
9.60	4.99(3.64)	3.55(2.58)	3.55(2.58)
13.43	8.93(6.51)	5.94(4.32)	5.94(4.32)

model. This falls in line with the hypothesis that, for pathological values of IR, pathological areas of pressure start to appear in the AJ. Despite being more common the appearance of medial degenerative areas in the ankle cartilage, the presence of lateral injuries was also described by Hirose et al. and Bischof et al. [28, 29], validating the lateral pressure felt by the posterolateral areas of the talar cartilage and by the fibular cartilage. The lesion of the lateral ligaments and consequent ankle rotational instability induces a laxity state on the AJ, raising the probability of cartilaginous injury caused by the appearance of the pathological pressure patterns mentioned earlier.

The results obtained for the ligamentous strains suggest that only the PTTL and the ATFL work against the movement of IR. In fact, there are multiple factors that can influence the stretching or shortening of ligaments on the IR. One of them is described by both Rasmussen [15] and Colville et al. [30] which is the ankle position before IR. In his work, Rasmussen claimed that the ATFL seemed to be the essential structure in restricting the IR, founding ruptures of this ligament whenever a forced IR was applied. The CFL, although being initially thought to be also a major antagonist of IR, is described by Rasmussen to not have a big influence on this movement when the ankle is in a neutral position. However, for an adducted - or inverted - ankle, the CFL is highly recruited, with ruptures of this ligament being found for a forced IR, and the same importance for a dorsiflexed ankle - without IR. The PTFL is also thought of limiting the IR, but Rasmussen found that its influence was circumscribed to an IR of an adducted ankle, having no major influence nor straining in a neutral ankle IR. This findings are in line with the computed strains obtained from the FE model. One of the main questions posed by Rasmussen was if the PTTL had any influence in forced IR. In fact, it was reported by Dehne [31] that the PTTL was stretched at the same time as the ATFL in forced IR, implying that it would possibly prevent that movement, thus being important in the control of rotatory instability.

Colville et al. [30] measured the LCL strains for the IR of the ankle for a range of flexion of the ankle - from 20°of plantarflexion to a neutral position and then to 20°of dorsiflexion - and found that both the CFL and the PTFL have little to no strain in a neutral ankle IR, whereas the ATFL had almost 10% of strain. The variations from the medical findings to the FE model results could be explained due to the ligament position on the model. For example, in the FE model, the CFL shortens, while in the *in vivo* experiments it has a minimal stretching, despite having low importance in the IR as stated above. The modelling of ligaments with a single truss instead of with multiple trusses representing the multiple fibers that compose them [32], along with a possible high sensitivity to the orientation of modelling, as explained above, represent major limitations of this work. Also, the axis of rotation could be inducing some degree of abduction - instead of a pure rotation - which, as also documented by Rasmussen and Colville et al. [15, 30], relieves some tension from the CFL and could be the cause of the ligament being shortened instead of stretched.

The extracted strains from the FE model are considered to be in line with the medical *in vivo* descriptions of ligament activation for a neutral internal rotated ankle. The ligament position in the FE model should, nevertheless, be better assessed with a sensitivity analysis.

The analysis and understanding of the reaction moments as a function of not only the IR angle, but also of the ligamentous configuration is important to assess ligamentous function and ankle instability. In fact, Cawley et al. [33] evaluated the effects of axial loads and single plane motions on ligament strain patterns and measured IR reaction torques for an intact ankle with and without the presence of an axial load - 650 N - and for all the possible ankle movements - DF, PF, inversion, eversion, IR and external rotation. Cadaveric feet were attached to a force platform and strain transducers were attached to the ATFL and to the CFL. Focusing on the IR tested, an angle of 15°was applied to an neutral ankle, and the values of the torque were of 5.7±5.06 N m for the IR without an axial load and of 9.7±4.2 N m with the presence of an axial load.

Although in the FE model a compressive axial force of 10 N is applied and the maximum rotational angle applied is not the same, considering the value of the reaction moment for an angle of IR of 13.43°applied in an intact ligamentous configuration, the value of 8.93 still falls into the range of values of the first case described by Cawley et al. without an axial load. It is also stated by Cawley et al. that the presence of an axial load leads to an higher reaction moment due to the fact that surface contact provides an increased resistance to IR. This happens due to the anatomy of both the talus and the tibial articular cages, which force some degree of external rotation, straining even more the ATFL. This data is particularly important for rehabilitation of injured ligaments, since by knowing the effects of the ankle position and of the axial load on ligament strain and ankle reaction torque, rehabilitation protocols can be improved, as well as the development of new orthotic devices.

Six years before, Stormont et al. [34] established the percentage change in torque with sectioning of

lateral ligaments, by using cadaveric ankles and applying inversion, eversion, IR and external rotation for a neutral ankle, a 20°plantar flexed ankle and a 20°dorsiflexed ankle. Comparing the percentage change in torque obtained for an IR after the sectioning of the ATFL measured by Stormont et al. - 7% -, and the difference between the normalized reaction moments for the intact ligaments and after the cut of the ATFL for an angle of 3.67°, the values support the hypothesis that for a neutrally placed ankle, the contribution of the ATFL is higher when compared with the contribution of, for example, the PTTL. This happens since for the same IR angle, the ATFL has a higher strain and the reaction moment increases quicker when the ATFL is modelled than when it is cut. Stormont et al. postulated then that the IR for a neutral ankle without any kind of loading has two main restraints, the ATFL and the PTTL, and that under loading, the articular surface becomes as important as the ligament restraint, when it comes to ankle stability [34].

To conclude, the reaction moments measured are an important tool to understand the main restraints of ankle stability, with the ATFL and the PTTL being two of the most important ligaments in the control of ankle IR, and the articular surface as a third restraint, even more for a loaded ankle and after ligamentous injury. This third restraint is a valuable information to understand the cartilaginous injury mechanism after ligamentar rupture.

5. Conclusions

This work determined the contact patterns for the 3 rotational situations described. The results showed not only an increase in the maximum pressure in the cartilage, but also but also is notorious the occurrence of anteromedial and posterolateral spots of pressure. These spots of pressure can be directly connected to cartilage degeneration and are a computational evidence that links the LCL injury to pathological cartilaginous pressures. In particular, the maximum pressures rised from 3.114 MPa to 4.770 MPa in the talar cartilage. To the author's knowledge, no documented values of contact pressure are described in the literature. However, the peak stresses on the talar cartilage were also extracted from the FE model and compared with the literature, showing that in this model a submaximal stress is observed in the cartilage. This submaximal stress can, nevertheless, induce cartilaginous injury through a cycled loading of the cartilage surface, as it has been documented by Brand [35]. However one of the main limitations of this work is that the axial load applied in the ankle joint is only used to accommodate the cartilaginous surfaces and cannot be considered as biological. Hence, every stress or pressure felt by the cartilage is likely to be submaximal when compared to other works that use biological loadings. The results taken from the FE model can, nonetheless, be a starting point to the understanding of cartilage damage in unstable ankles.

The ligamentous strains were also analyzed in this work to understand the importance of the ligamentar structure not only in the control of the foot, but also to evaluate the influence on the cartilaginous pressures measured. In fact, it was perceived that both the ATFL and the PTTL had high strains when compared with the other ligaments. This ligamentar activation follows what is present in the available literature, only having differences in the CFL strains. This ligament is thought to have little importance in the IR, but still having some degree of strain. However, in this work, the CFL shortens, denoting that either the orientation of the ligament could not be the ideal or that the movement of the ankle could also have some degree of abduction - which is known to shorten the CFL.

Lastly, the reaction moments were evaluated and compared to the ones present in the literature, with the values extracted from the FE model growing with the increase of the rotation magnitude and lowering with the cut of the ATFL since this ligament opposes the IR. The lack of strain of the CFL explains the same reaction moment for the same angle for the last two ligamentar configurations considered. By comparing the values retrieved from the FE model for the reaction moments with the literature available, it can be noticed that both the ATFL and the PTTL are the two main restraints to IR, highly influencing the reaction moment of the ankle. The articular cartilage is also an important restraint, possibly explaining why the damage is higher after ligamentar injury.

It is important to mention that, to the authors knowledge, this is the only FE study in the literature that focuses on ankle rotation, meaning that this thesis can be a basis for future research on rotational instability and cartilaginous injury. The weaknesses of this study are discussed in the next section and, if addressed properly, can help on the better understanding of the rotational behavior of the ankle.

References

[1] P. A. Houglum and D. B. Bertoti, *Brunnstorm's Clinical Kinesiology*. F.A. Davis, 6 ed., 2012.

[2] D. T. P. Fong, Y. Hong, L. K. Chan, P. S. H. Yung, and K. M. Chan, "A systematic review on ankle injury and ankle sprain in sports," *Sports Medicine*, vol. 37, no. 1, pp. 73–94, 2007.

[3] S. L. Haddad, "Sprained Ankle," 2016.

[4] F. Guerra-Pinto, N. Côrte-Real, T. Mota Gomes, M. D. Silva, J. G. Consciência, M. Monzo, and X. M. Oliva, "Rotational Instability after Anterior Talofibular and Calcaneofibular Ligament Section: The Experimental Basis for the Ankle Pivot Test," *Journal of Foot and Ankle Surgery*, 2018.

[5] C. L. Saltzman, M. L. Salamon, G. M. Blanchard, T. Huff, A. Hayes, J. a. Buckwalter, and A. Amendola, "Epidemiology of ankle arthritis: report of a consecutive series of 639 patients from a tertiary orthopaedic center.," *The Iowa orthopaedic journal*, vol. 25, pp. 44–6, 2005.

[6] Phone, "Osteoporosis and Arthritis: Two Common but Different Conditions," *Bone*, no. April, pp. 202–223, 2015.

[7] K. D. Harrington, "Degenerative arthritis of the ankle secondary to long-standing lateral ligament instability.," *The Journal of Bone & Joint Surgery*, vol. 61, pp. 354–361, 4 1979.

[8] P. E. Scranton, J. E. Mcdarmott, and J. V. Rogers, "The Relationship between Chronic Ankfe Instability and Variations in Mortise Anatomy and ImpEngement Spurs," *Orthopedics*, vol. 21, pp. 657–664, 2000.

[9] I. Taga, K. Shino, M. Inoue, K. Nakata, A. Maeda, and J. H. Henry, "Articular cartilage lesions in ankles with lateral ligament injury. An arthroscopic study," *American Journal of Sports Medicine*, vol. 21, pp. 120–127, 1 1993.

[10] W. Petersen, I. V. Rembitzki, A. G. Koppenburg, A. Ellermann, C. Liebau, G. P. Brüggemann, and R. Best, "Treatment of acute ankle ligament injuries: A systematic review," *Archives of Orthopaedic and Trauma Surgery*, vol. 133, no. 8, pp. 1129–1141, 2013.

[11] H. Zwipp, R. Hoffmann, H. Thermann, and B. W. Wippermann, "Rupture of the ankle ligaments," *International Orthopaedics*, vol. 15, no. 3, pp. 245–249, 1991.

[12] C. N. Van Dijk, B. W. J. Mol, L. S. Lim, R. K. Marti, and P. M. Bossuyt, "Diagnosis of ligament rupture of the ankle joint: Physical examination, arthrography, stress radiography and sonography compared in 160 patients after inversion trauma," *Acta Orthopaedica*, vol. 67, no. 6, pp. 566–570, 1996.

[13] T. Golditz, S. Steib, K. Pfeifer, M. Uder, K. Gelse, R. Janka, F. F. Hennig, and G. H. Welsch, "Functional ankle instability as a risk factor for osteoarthritis: Using T2-mapping to analyze early cartilage degeneration in the ankle joint of young athletes," *Osteoarthritis and Cartilage*, vol. 22, no. 10, pp. 1377–1385, 2014.

[14] P. Cignoni, P. Cignoni, M. Callieri, M. Callieri, M. Corsini, M. Corsini, M. Dellepiane, M. Dellepiane, F. Ganovelli, F. Ganovelli, G. Ranzuglia, and G. Ranzuglia, "MeshLab: an Open-Source Mesh Processing Tool," *Sixth Eurographics Italian Chapter Conference*, pp. 129–136, 2008.

[15] O. Rasmussen, *Stability of the Ankle Joint*, vol. 56. 1985.

[16] F. Corazza, J. J. O'Connor, A. Leardini, and V. P. Castelli, "Ligament fibre recruitment and forces for the anterior drawer test at the human ankle joint," *Journal of Biomechanics*, vol. 36, no. 3, pp. 363–372, 2003.

[17] A. S.Kelikian and S. K. Sarrafian, *Sarrafian's Anatomy of the Foot and Ankle: Descriptive, Topographic, Functional.* 3rd ed., 2011.

[18] J. T.-m. Cheung and M. A. Zhang, "A 3-Dimensional Finite Element Model of the Human Foot and Ankle for Insole Design," vol. 86, no. February, 2005.

[19] A. Gefen, M. Megido-Ravid, Y. Itzchak, and M. Arcan, "Biomechanical Analysis of the Three-Dimensional Foot Structure During Gait: A Basic Tool for Clinical Applications," *Journal of Biomechanical Engineering*, vol. 122, no. 6, p. 630, 2000.

[20] Z. Xu-shu, G. U. O. Yuan, and C. Wei-yi, "3-D Finite Element Method Modeling and Contact Pressure Analysis of the Total Knee Joint in Flexion," *In Vivo*, no. Nsfc 10702048, pp. 8–10, 2009.

[21] P. C. Liacouras and J. S. Wayne, "Computational Modeling to Predict Mechanical Function of Joints: Application to the Lower Leg With Simulation of Two Cadaver Studies," *Journal of Biomechanical Engineering*, vol. 129, no. 6, p. 811, 2007.

[22] S. Siegler, J. Block, and C. D. Schneck, "The mechanical characteristics of the collateral ligaments of the human ankle joint," *Foot & ankle*, vol. 8, no. 5, pp. 234–242, 1988.

[23] M. Ozen, O. Sayman, and H. Havitcioglu, "Modeling and stress analyses of a normal foot-ankle and a prosthetic foot-ankle complex," *Acta of Bioengineering and Biomechanics*, vol. 15, no. 3, pp. 19–27, 2013.

[24] B. A. Hills and B. D. Buttler, "Surfactants identified in synovial fluid and their ability to act as boundary lubricants," *Annals of the Rheumatic Diseases*, vol. 43, no. 4, pp. 641–648, 1984.

[25] S. C. Tadepalli, A. Erdemir, and P. R. Cavanagh, "Comparison of hexahedral and tetrahedral elements in finite element analysis of the foot and footwear," *Journal of Biomechanics*, vol. 44, no. 12, pp. 2337–2343, 2011.

[26] J. P. Arokoski, J. S. Jurvelin, U. Väätäinen, and H. J. Helminen, "Normal and pathological adaptations of articular cartilage to joint loading," *Scandinavian Journal of Medicine and Science in Sports*, vol. 10, no. 4, pp. 186–198, 2000.

[27] L. A. Setton, D. M. Elliott, and V. C. Mow, "Altered mechanics of cartilage with osteoarthritis: Human osteoarthritis and an experimental model of joint degeneration," *Osteoarthritis and Cartilage*, vol. 7, no. 1, pp. 2–14, 1999.

[28] K. Hirose, G. Murakami, T. Minowa, H. Kura, and T. Yamashita, "Lateral ligament injury of the ankle and associated articular cartilage degeneration in the talocrural joint: Anatomic study using elderly cadavers," *Journal of Orthopaedic Science*, vol. 9, no. 1, pp. 37–43, 2004.

[29] J. E. Bischof, C. E. Spritzer, A. M. Caputo, M. E. Easley, J. K. DeOrio, J. A. Nunley, and L. E. DeFrate, "In vivo cartilage contact strains in patients with lateral ankle instability," *Journal of Biomechanics*, vol. 43, no. 13, pp. 2561–2566, 2010.

[30] M. R. Colville, R. A. Marder, J. J. Boyle, and B. Zarins, "Strain measurement in lateral ankle ligaments," *The American Journal of Sports Medicine*, vol. 18, no. 2, pp. 196–200, 1990.

[31] E. Dehne, "Die Klinik der frischen und habituellen Adduktionssupinationsdistorsion des Füßes," *Langenbeck's Archives of Surgery*, vol. 242, no. 1, pp. 40–60, 1933.

[32] R. Drake, W. Vogl, and A. Mitchell, *Gray's Anatomy for Students*. 2009.

[33] P. W. Cawley and E. P. France, "Biomechanics of the lateral ligaments of the ankle: An evaluation of the effects of axial load and single plane motions on ligament strain patterns," *Foot and Ankle*, vol. 12, no. 2, pp. 92–99, 1991.

[34] D. M. Stormont, B. F. Morrey, K. N. an, and J. R. Cass, "Stability of the loaded ankle:Relation between articular restraint and primary and secondary static restraints," *The American Journal of Sports Medicine*, vol. 13, no. 5, pp. 295–300, 1985.

[35] R. A. Brand, "Joint Contact Stress: a Reasonable Surrogate for Biological Processes?," *The Iowa Orthopaedic Journal*, vol. 25, pp. 82–94, 2005.